

Article

Deep-Learning Algorithms for Prescribing Insoles to Patients with Foot Pain

Jeoung Kun Kim ¹, Yoo Jin Choo ² , In Sik Park ³, Jin-Woo Choi ⁴, Donghwi Park ^{4,*} 
and Min Cheol Chang ^{2,*} 

¹ Department of Business Administration, School of Business, Yeungnam University, Gyeongsan-si 38541, Republic of Korea

² Department of Physical Medicine and Rehabilitation, Yeungnam University Medical Center, College of Medicine, Yeungnam University, 317-1 Daemyungdong, Namku, Daegu 41415, Republic of Korea

³ Korean Podiatry and Pedorthics Institute, Goyang 10442, Republic of Korea

⁴ Department of Physical Medicine and Rehabilitation, University of Ulsan College of Medicine, Ulsan University Hospital, 877 Bangeojin Sunhwando-ro, Dong-gu, Ulsan 44033, Republic of Korea

* Correspondence: bdome@hanmail.net (D.P.); wheel633@ynu.ac.kr (M.C.C.); Tel.: +82-52-250-7222 (D.P.); +82-53-620-4682 (M.C.C.); Fax: +82-52-250-7228 (D.P.)

† These authors contributed equally to this work.

Abstract: Foot pain is a common musculoskeletal disorder. Orthotic insoles are widely used in patients with foot pain. Inexperienced clinicians have difficulty prescribing orthotic insoles appropriately by considering various factors associated with the alteration of foot alignment. We attempted to develop deep-learning algorithms that can automatically prescribe orthotic insoles to patients with foot pain and assess their accuracy. In total, 838 patients were included in this study; 70% (n = 586) and 30% (n = 252) were used as the training and validation sets, respectively. The resting calcaneal stance position and data related to pelvic elevation, pelvic tilt, and pelvic rotation were used as input data for developing the deep-learning algorithms for insole prescription. The target data were the foot posture index for the modified root technique and the necessity of heel lift, entire lift, and lateral wedge, medial wedge, and calcaneocuboid arch supports. In the results, regarding the foot posture index for the modified root technique, for the left foot, the mean absolute error (MAE) and root mean square error (RMSE) of the validation dataset for the developed model were 1.408 and 3.365, respectively. For the right foot, the MAE and RMSE of the validation dataset for the developed model were 1.601 and 3.549, respectively. The accuracies for heel lift, entire lift, and lateral wedge, medial wedge, and calcaneocuboid arch supports were 89.7%, 94.8%, 72.2%, 98.4%, and 79.8%, respectively. The micro-average area under the receiver operating characteristic curves for heel lift, entire lift, and lateral wedge, medial wedge, and calcaneocuboid arch supports were 0.949, 0.941, 0.826, 0.792, and 0.827, respectively. In conclusion, our deep-learning models automatically prescribed orthotic insoles in patients with foot pain and showed outstanding to acceptable accuracy.

Keywords: insole; foot pain; deep learning; prescription



check for updates

Citation: Kim, J.K.; Choo, Y.J.; Park, I.S.; Choi, J.-W.; Park, D.; Chang, M.C. Deep-Learning Algorithms for Prescribing Insoles to Patients with Foot Pain. *Appl. Sci.* **2023**, *13*, 2208. <https://doi.org/10.3390/app13042208>

Academic Editors: Levente Adalbert Kovács and László Szilágyi

Received: 17 November 2022

Revised: 7 February 2023

Accepted: 7 February 2023

Published: 9 February 2023



Copyright: © 2023 by the authors. Licensee MDPI, Basel, Switzerland. This article is an open access article distributed under the terms and conditions of the Creative Commons Attribution (CC BY) license (<https://creativecommons.org/licenses/by/4.0/>).

1. Introduction

Foot pain is common among adults and is frequently observed in patients who visit pain clinics, particularly older adults [1,2]. Its prevalence among adults aged ≥ 18 years is reported to range from 17 to 24% [3]. It can lead to a diminished ability to perform activities of daily living, problems with balance and gait, and an increased risk of falls [1,2]. Foot pain is reported to significantly impact the quality of daily life and work [1,2]. Therefore, the appropriate treatment of foot pain is important. Despite the use of various therapeutic methods such as oral medication, physical therapy, injections, extracorporeal shockwave therapy, and orthoses, many patients frequently complain of persistent foot pain [1,2,4,5]. The development of foot pain is associated with alterations in foot alignment, which result

in abnormally distributed loads on the foot [6,7]. Orthotic insoles are frequently used to correct altered foot alignments [8,9]. The usefulness of orthotic insoles for patients with foot pain has been demonstrated in several previous studies, and they have been widely applied in clinical practice for the treatment of foot pain [10–12].

Additionally, the asymmetrical motion between the right and left lower limbs and pelvic malalignment is kinetically associated with abnormal foot motion [13]. A misalignment can create excessive load on certain foot structures, causing foot pain. To correct the symmetry between the lower limbs and pelvic malalignment, the height of orthotic insoles can be adjusted by lifting the insole. The asymmetric movement of the pelvis can be corrected by applying lateral wedge, medial wedge, and calcaneocuboid arch supports to the insole and lifting the heel [14,15]. The rotation of the pelvis to one side can be blocked using lateral wedge, medial wedge, and calcaneocuboid arch supports. The tilt of one side of the pelvis toward the anterior region can be corrected by a heel lift.

A lot of experience should be accumulated to prescribe orthotic insoles appropriately. To apply the appropriate orthotic insole, clinicians should consider various factors such as foot alignment, pelvic movement, and leg length discrepancy [13,16]. The comprehensive consideration of various factors associated with the alteration of foot alignment is difficult for inexperienced clinicians. An algorithm that automatically prescribes the orthotic insole would be of great help to clinicians treating patients with foot pain.

Machine learning is an artificial intelligence technique that involves system learning rules and patterns from given data [17–19]. It has several advantages for determining the appropriate prescription for patients with various disorders [17–19]. The deep-learning technique is an advanced machine learning approach [20,21]. In particular, it constructs artificial neural networks with functions and structures similar to those of the human brain using a large number of hidden layers [20,21]. Several studies have demonstrated that the deep-learning technique can outperform traditional machine learning techniques [17–19].

We propose that deep learning can be used to develop an algorithm that automatically prescribes orthotic insoles to patients with foot pain, using several measured results as input data. In the current study, we investigated the potential of deep learning to prescribe an appropriate orthotic insole for patients with foot pain.

2. Methods

2.1. Study Design and Population

The data for developing the machine learning algorithms were obtained from a single insole manufacturer (BioMechanics, Goyang-si, Republic of Korea). Insoles were made on the basis of the insole prescription paper on which the results of the physical examination, including the resting calcaneal stance position (RCSP), pelvic elevation, pelvic tilt, and pelvic rotation, were written [22–24]. The prescription paper was written by a podiatrist (ISP) who had more than 25 years of experience in the prescription of orthotic insoles for patients with foot pain. Insole prescriptions were written at five different hospitals. We used the following inclusion criteria: (1) age \geq 20 years, (2) the insole was prescribed for managing foot pain, (3) patients with no neurological disorders, (4) patients with no diabetic foot ulcer, and (5) the presence of an insole prescription paper containing all the information on the RCSP, pelvic elevation, pelvic tilt, and pelvic rotation.

Informed consent was waived by the Institutional Review Board of Yeungnam University Hospital. This study was approved by the Institutional Review Board of Yeungnam University Hospital (2022-06-046). All procedures were carried out in accordance with the relevant guidelines and regulations.

2.2. Input Variables

Resting Calcaneal Stance Position

To measure the RCSP, patients with foot pain were asked to place their foot on the edge of the bed and lay in the prone position on a bed parallel to the ground. The investigator manually inspected the foot and drew a bisector by placing three dots on the top, middle, and bottom of the heel, regardless of the fat surrounding the calcaneus (Figure 1A). The RCSP was measured when the patients stood on their feet placed at a fist-width distance (Figure 1B). Angles were determined between the line of the heel and the surface.



Figure 1. Measurement of the resting calcaneal stance position (RCSP), pelvic elevation, pelvic tilt, and pelvic rotation. Measurements of the (A) RCSP in the prone position, (B) RCSP in the standing position, (C) pelvic elevation, (D,E) pelvic tilt, and (F) pelvic rotation.

2.3. Pelvic Elevation, Pelvic Tilt, and Pelvic Rotation

Pelvic elevation indicated the height difference between the left and right iliac crests. It was measured using an angulometer with the patients standing on their feet placed at a fist-width distance. The right and left blades of the angulometer were placed at the highest point of the iliac crest, and pelvic elevation was measured (Figure 1C). When one iliac crest was elevated relative to the iliac crest of the other side, the value was indicated as a positive value, and a larger value indicated a greater difference in the heights of the left and right pelvis (e.g., when the heights of the left and right iliac crests were the same, it was described as 0-0, and when the height of the left iliac crest was 2 degrees higher than the other side, it was presented as 2-0).

To assess the presence of pelvic tilt, the investigator's thumb was placed on the posterior superior iliac spine (PSIS), and the remaining fingers were placed on the patient's iliac crest (Figure 1D). The investigator then asked the patients to bend their lower back 90 degrees forward and assessed the difference in the degree of anterior tilt of the investigator's thumb (Figure 1E). When the tilt of both PSISs was symmetrical, it was presented as "−,−," and when the tilt of the left PSIS was greater than the left PSIS, it was presented as "+,−."

To measure pelvic rotation, the investigator attached the angulometer to the patients' PSISs, asked the patients to walk in place, and observed the movement of the angulometer (Figure 1F). The investigator assessed whether the degree of the backward movement of the right and left wings of the angulometer was symmetrical. When the angulometer attached to the patients' PSIS moved backward symmetrically, it was described as “-,-,” and when the left side moved backward more than the right side, it was described as “+,-.”

2.4. Target Variables

The foot posture index for the modified root technique and the application of heel lift, entire lift, and lateral wedge, medial wedge, and calcaneocuboid arch supports were set as the target variables (Figure 2).

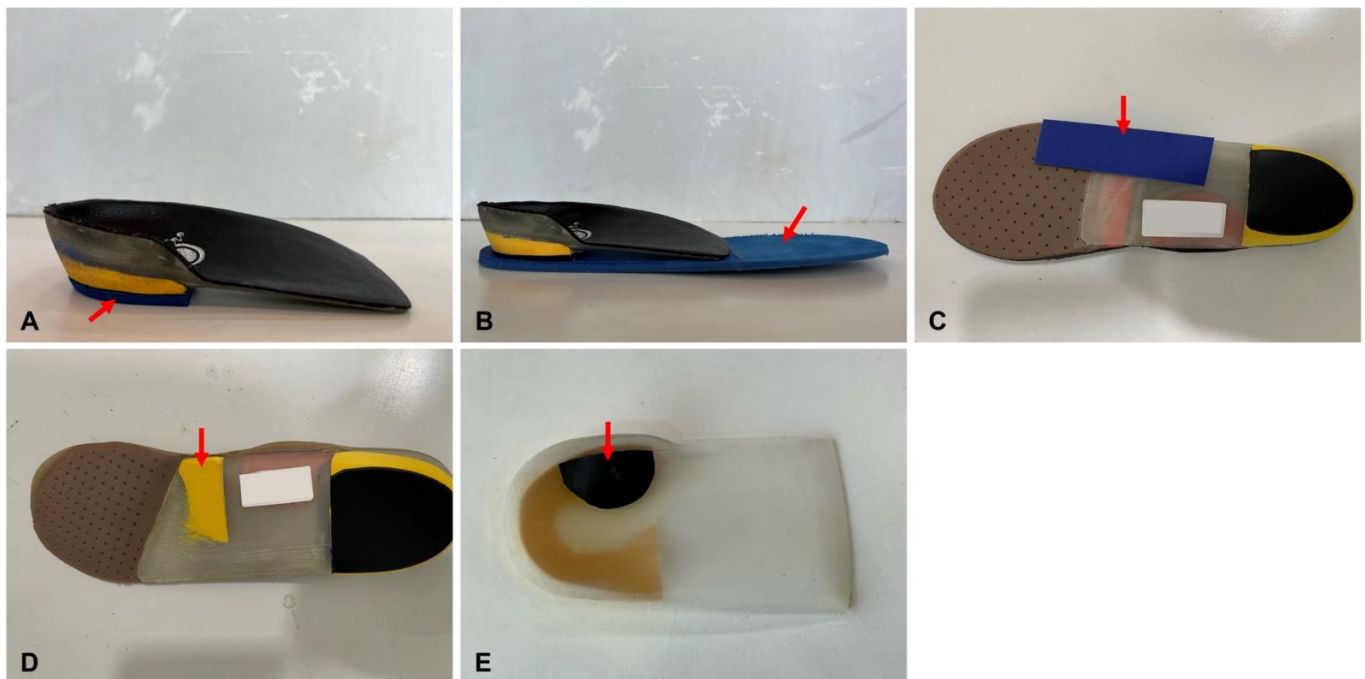


Figure 2. Photographs of (A) heel lift, (B) entire lift, and (C) lateral wedge, (D) medial wedge, and (E) calcaneocuboid arch supports.

2.5. Deep-Learning Algorithms

Sequential deep neural networks (DNNs) were applied for classification and sequential DNN-based regression algorithms (Supplementary Materials). TensorFlow 2.9.1 with Keras, Python 3.8.1, and Scikit-learn 1.1.1. were used to train two DNN regression models (right and left feet) for automatic prescriptions of the foot posture index for the modified root technique and five DNN classification models to determine the application of heel lift, entire lift, and lateral wedge, medial wedge, and calcaneocuboid arch supports. Among the study population, 70% ($n = 586$) and 30% ($n = 252$) were included in the training and validation sets, respectively. The details of each model are listed in Tables 1–6.

Table 1 shows the application of deep-learning regression to determine the foot posture index. This approach is particularly effective because of its capability to handle complex and non-linear associations between inputs and outputs, making it an optimal solution for determining the foot posture index using continuous values. The mean absolute error (MAE) and root mean square error (RMSE) were used to validate the performance of the two regression models.

Table 1. Details of the model for determining the foot posture index for the modified root technique.

	Prescription Left DNN Regression Model	Prescription Right DNN Regression Model
DNN model	<ul style="list-style-type: none"> - Four hidden layers with 256-128-128-64 neurons - RMSProp optimizer, ReLU activation - Learning rate 1×10^{-5}, batch size 512 - Batch normalization for regularization 	<ul style="list-style-type: none"> - Five hidden layers with 512-512-1024-1024-512 neurons - RMSProp optimizer, ReLU activation - Learning rate 2×10^{-3}, batch size 512 - Batch normalization for regularization
Model performance	<ul style="list-style-type: none"> - MAE 1.460, RMSE 3.539 for training - MAE 1.408, RMSE 3.365 for validation 	<ul style="list-style-type: none"> - MAE 1.560, RMSE 3.860 for training - MAE 1.601, RMSE 3.549 for validation

DNN, deep neural network; RMSProp, root mean squared propagation; ReLU, rectified linear unit; MAE, mean absolute error; RMSE, root mean square error.

Table 2. Details of the model for determining the application of heel lift.

Sample size and ratio Sample class size and ratio	<ul style="list-style-type: none"> - 70% for training: 586; 30% for validation: 252; total: 838 - Class 0: 392 (66.9%), class 1: 64 (10.9%), class 2: 130 (22.2%) for training - Class 0: 169 (67.1%), class 1: 28 (11.1%), class 2: 55 (21.8%) for validation 					
DNN model	<ul style="list-style-type: none"> - Five hidden layers with 512-512-1024-1024-512 neurons - Adam optimizer, ReLU activation - Learning rate 1×10^{-2} batch size 32 - Dropout layer for regularization - Training accuracy: 89.1%, validation accuracy: 89.7% 					
Model performance (validation data)	Class	Precision	Recall	F1-score	Support	ROC AUC
	0	0.961	0.882	0.920	169	0.942
	1	0.839	0.939	0.881	28	0.993
	2	0.773	0.927	0.843	55	0.950
	Macro average	0.858	0.913	0.881	252	0.961
	Micro average	0.907	0.897	0.899	252	0.949

DNN, deep neural network; Adam, adaptive moment estimation; ReLU, rectified linear unit; ROC, receiver operating characteristic; AUC, area under the curve; class 0, no application; class 1, application of heel lift to the right side; class 2, application of heel lift to the left side.

Table 3. Details of the model for determining the application of entire lift.

Sample size and ratio Sample class size and ratio	<ul style="list-style-type: none"> - 70% for training: 586; 30% for validation: 252; total: 838 - Class 0: 508 (86.7%), class 1: 23 (3.9%), class 2: 55 (9.4%) for training - Class 0: 218 (86.5%), class 1: 10 (4%), class 2: 24 (9.5%) for validation 					
DNN model	<ul style="list-style-type: none"> - Three hidden layers with 256-256-512 neurons - RMSProp optimizer, ReLU activation - Learning rate 5×10^{-3}, batch size 2 - Dropout layer for regularization - Training accuracy: 94.7%, validation accuracy: 94.8% 					
Model performance (validation data)	Class	Precision	Recall	F1-score	Support	ROC AUC
	0	0.977	0.968	0.972	218	0.939
	1	0.750	0.600	0.667	10	0.868
	2	0.786	0.917	0.846	24	0.991
	Macro average	0.838	0.828	0.828	252	0.933
	Micro average	0.950	0.948	0.948	252	0.941

DNN, deep neural network; RMSProp, root mean squared propagation; ReLU, rectified linear unit; ROC, receiver operating characteristic; AUC, area under the curve; class 0, no application; class 1, application of entire lift to the right side; class 2, application of entire lift to the left side.

Table 4. Details of the model for determining the application of lateral wedge support.

Sample size and ratio Sample class size and ratio	- 70% for training: 586; 30% for validation: 252; total: 838 - Class 0: 571 (97.4%), class 1: 9 (0.015%), class 2: 3 (0.005%), class 3: 3 (0.005%) for training - Class 0: 245 (97.2%), class 1: 4 (0.016%), class 2: 1 (0.004%), class 3: 2 (0.008%) for validation					
DNN model	- Two hidden layers with 256-1024 neurons - RMSProp optimizer, ReLU activation - Learning rate 5×10^{-4} , batch size 128 - Dropout layer for regularization - Training accuracy: 98.8%, validation accuracy: 98.4%					
Model performance (validation data)	Class	Precision	Recall	F1-score	Support	ROC AUC
	0	0.988	0.996	0.992	245	0.790
	1	0.667	0.500	0.571	4	0.861
	2	1.000	1.000	1.000	1	1.000
	3	1.000	0.500	0.667	2	0.800
	Macro average	0.914	0.749	0.807	252	0.863
Micro average	0.983	0.984	0.983	252	0.792	
DNN, deep neural network; RMSProp, root mean squared propagation; ReLU, rectified linear unit; ROC, receiver operating characteristic; AUC, area under the curve; class 0, no application; class 1, application of medial wedge support to the right side; class 2, application of medial wedge support to the left side; class 3, application of medial wedge support to both sides.						

Table 5. Details of the model for determining the application of medial wedge support.

Sample size and ratio Sample class size and ratio	- 70% for training: 586; 30% for validation: 252; total: 838 - Class 0: 289 (49.3%), class 1: 19 (3.2%), class 2: 80 (13.7%), class 3: 198 (33.8%) for training - Class 0: 124 (49.2%), class 1: 8 (3.2%), class 2: 35 (13.9%), class 3: 85 (33.7%) for validation					
DNN model	- Two hidden layers with 256-1024 neurons - Nadam optimizer, ReLU activation - Learning rate 5×10^{-5} , batch size 64 - Dropout layer for regularization - Training accuracy: 93.0%, validation accuracy: 72.2%					
Model performance (validation data)	Class	Precision	Recall	F1-score	Support	ROC AUC
	0	0.786	0.798	0.792	124	0.827
	1	0.333	0.250	0.285	8	0.754
	2	0.455	0.429	0.441	35	0.791
	3	0.759	0.776	0.767	85	0.845
	Macro average	0.583	0.583	0.572	252	0.804
Micro average	0.716	0.722	0.719	252	0.826	
DNN, deep neural network; Nadam, Nesterov-accelerated adaptive moment estimation; ReLU, rectified linear unit; ROC, receiver operating characteristic; AUC, area under the curve; class 0, no application; class 1, application of lateral wedge support to the right side; class 2, application of lateral wedge support to the left side; class 3, application of lateral wedge support to both sides.						

Tables 2–6 present the results of the multi-class classification models designed to handle more than two classes or categories. The entire lift, lateral wedge support, and calcaneocuboid arch support models used the RMSProp optimizer. The heel lift and medial wedge support models utilized the Adam and Nadam optimizers, respectively. In terms of performance, the heel lift, entire lift, and lateral wedge support models exhibited exceptional results, with accuracy rates surpassing 90% for the validation data. In contrast, the accuracies of the medial wedge support and calcaneocuboid arch support models were moderate, yielding accuracy levels ranging between 72% and 80% for the validation data.

Table 6. Details of the model for determining the application of calcaneocuboid arch support.

Sample size and ratio Sample class size and ratio	- 70% for training: 586; 30% for validation: 252; total: 838 - Class 0: 412 (70.3%), class 1: 36 (6.1%), class 2: 138 (23.6%) for training - Class 0: 177 (70.2%), class 1: 16 (6.4%), class 2: 59 (23.4%) for validation					
DNN model	- Four hidden layers with 1024-512-256-128 neurons - RMSProp optimizer, ReLU activation - Learning rate 2×10^{-3} , batch size 128 - Dropout layer for regularization - Training accuracy: 88.7%, validation accuracy: 79.8%					
Model performance (validation data)	Class	Precision	Recall	F1-score	Support	ROC AUC
	0	0.868	0.853	0.860	177	0.824
	1	0.684	0.812	0.743	16	0.859
	2	0.627	0.627	0.627	59	0.828
	Macro average	0.726	0.764	0.743	252	0.837
	Micro average	0.800	0.798	0.798	252	0.827

DNN, deep neural network; RMSProp, root mean squared propagation; ReLU, rectified linear unit; ROC, receiver operating characteristic; AUC, area under the curve; class 0, no application; class 1, application of calcaneocuboid arch support to the right side; class 2: application of calcaneocuboid arch support to the left side.

3. Statistical Analysis

Receiver operating characteristic (ROC) curve analysis was performed using scikit-learn, and the area under the curve (AUC) was calculated. The one-versus-one (OVO) method was used to calculate accurate multi-class macro- and micro-average ROC AUC values. The OVO method is a commonly used approach for solving multi-class imbalance problems; this method transforms a multi-class problem into a set of two-class sub-problems [25].

4. Results

In total, 838 patients (mean age, 47.7 ± 14.7 years; 323 men, 515 women) were included. Regarding the foot posture index for the modified root technique, for the left foot, the mean absolute error (MAE) and root mean square error (RMSE) of the validation dataset for the developed model were 1.408 and 3.365, respectively (Table 1). For the right foot, the MAE and RMSE of the validation dataset for the developed model were 1.601 and 3.549, respectively (Table 1). The accuracy of applying heel lift was 89.7%, and the macro- and micro-average ROC AUC values were 0.961 and 0.949, respectively (Figure 3A). The accuracy of applying entire lift was 94.8%, and the macro- and micro-average ROC AUC values were 0.933 and 0.941, respectively (Figure 3B). The accuracy of applying lateral wedge support was 72.2%, and the macro- and micro-average ROC AUC values were 0.804 and 0.826, respectively (Figure 3C). The accuracy of applying medial wedge support was 98.4%, and the macro- and micro-average ROC AUC values were 0.863 and 0.792, respectively (Figure 3D). The accuracy of applying calcaneocuboid arch support was 79.8%, and the macro- and micro-average ROC AUC values were 0.837 and 0.827, respectively (Figure 3E).

Figure 4 shows the correct classification and misclassification of the DNN models. The model for the application of heel lift and entire lift correctly classified 226 and 239 of 252 cases, respectively, from the validation dataset. The model for the application of medial and lateral wedge supports correctly classified 182 and 248 of 252 cases, respectively, from the validation dataset. Lastly, the model for the application of calcaneocuboid arch support correctly classified 201 of 252 cases from the validation dataset. It can be concluded that the overall classification accuracy of the five models is good. However, the medial wedge model (Figure 4D) has lower accuracy for classes 1 and 2 due to a small sample size of patients in the validation data for those classes, resulting in inadequate learning.

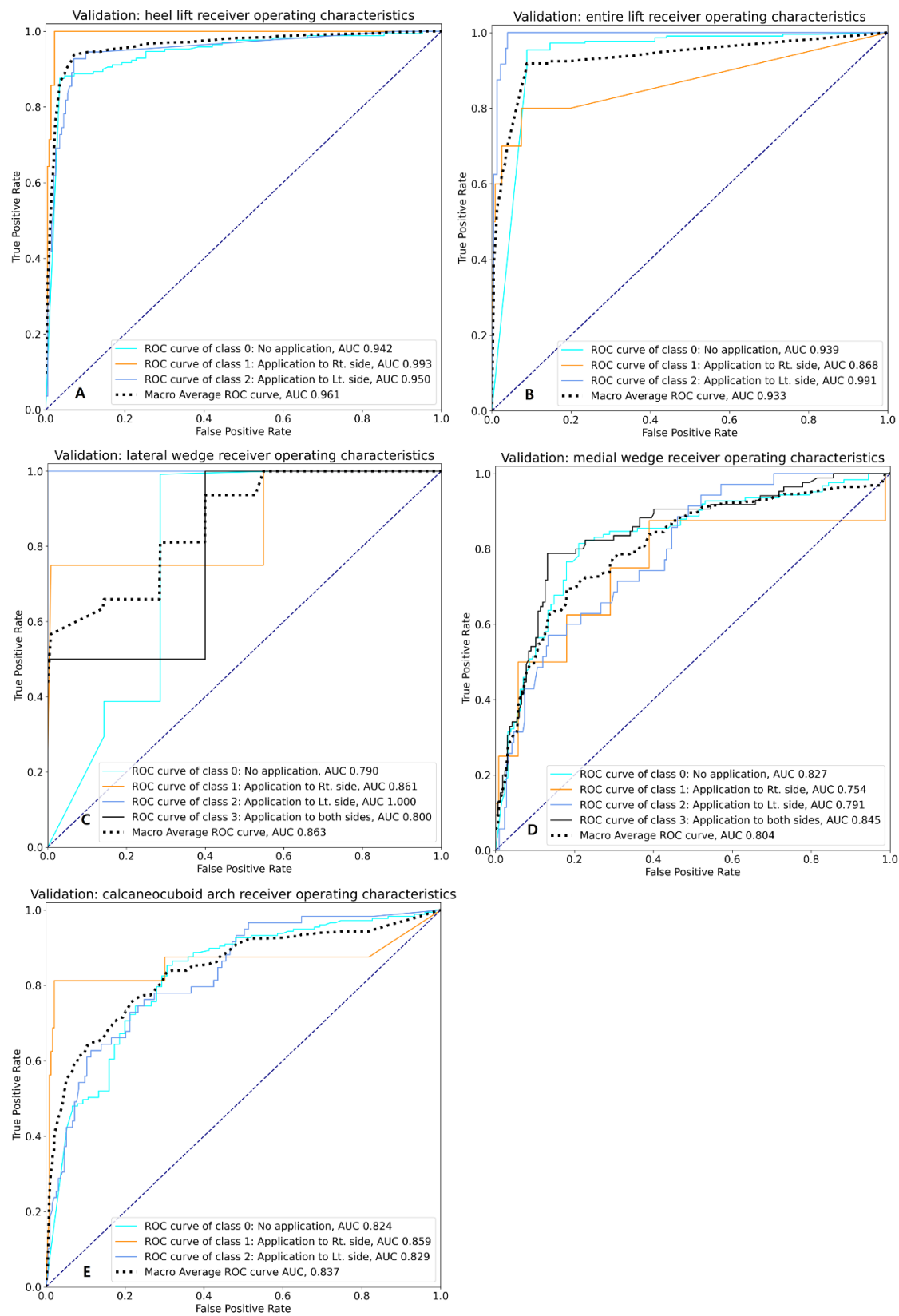


Figure 3. Receiver operating characteristic curve of the validation dataset of the deep-learning models for the prescription of orthotic insoles. (A) heel lift (B) entire lift (C) lateral wedge (D) medial wedge (E) calcaneocuboid arch.

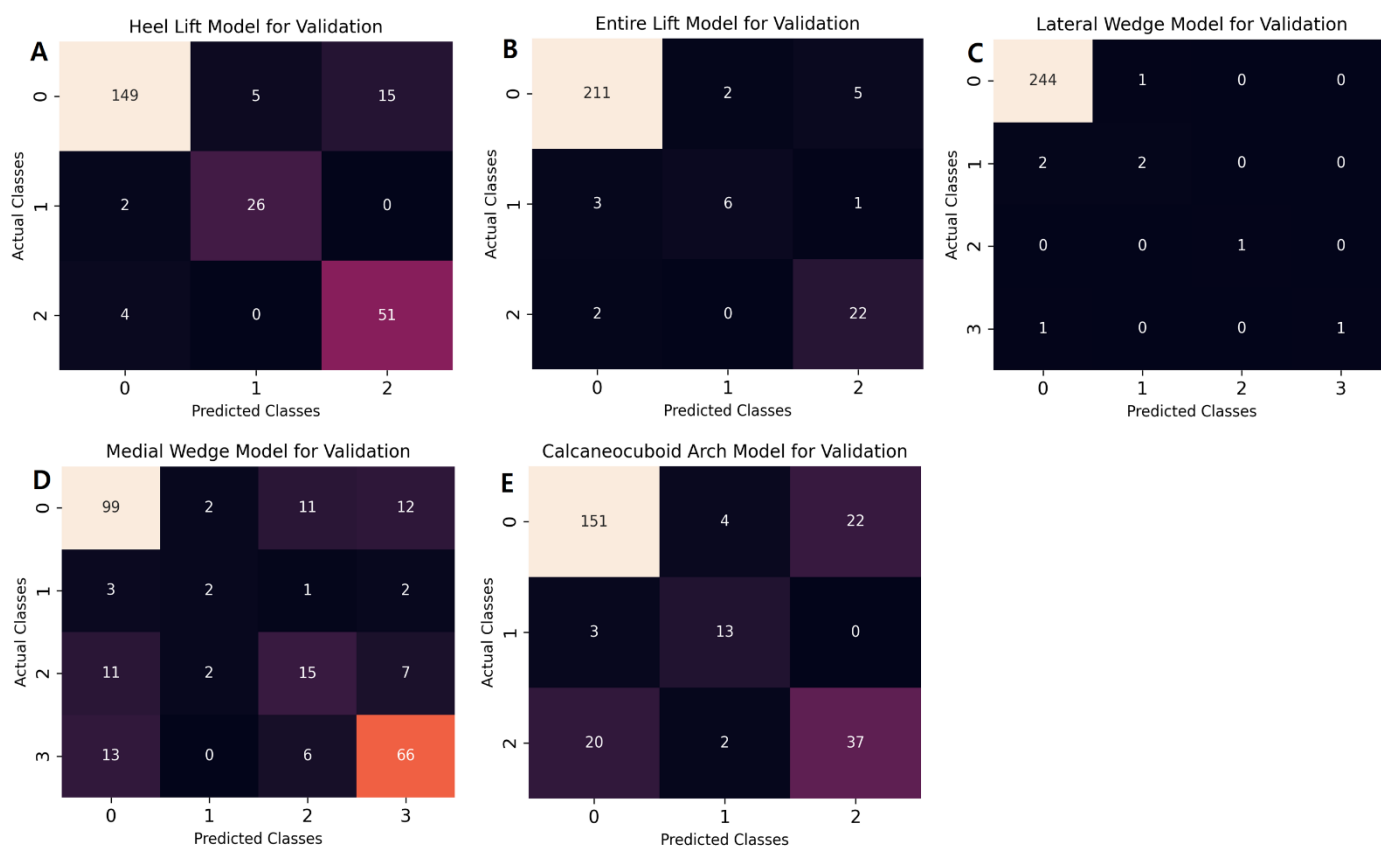


Figure 4. Confusion matrix of the deep-learning model for the prescription of orthotic insoles. (A) heel lift (B) entire lift (C) lateral wedge (D) medial wedge (E) calcaneocuboid arch.

5. Discussion

In this study, we developed a deep-learning model for prescribing the appropriate orthotic insole for patients with foot pain. Our developed model automatically determined the foot posture index for the modified root technique and the necessity of heel lift, entire lift, and lateral wedge, medial wedge, and calcaneocuboid arch supports. The MAE of the foot posture index for the modified root technique in our model was 1.6. The micro-average ROC AUC values of the models for determining the necessity of applying heel lift and entire lift were >0.9, and those of lateral wedge, medial wedge, and calcaneocuboid arch supports were 0.79–0.83. Considering that ROC AUC values ranging from 0.7 to 0.8 are considered acceptable, those ranging from 0.8 to 0.9 are considered excellent, and those >0.9 are considered outstanding. Therefore, these results indicate that the ability of our developed model to automatically prescribe orthotic insole ranged from outstanding to acceptable, which supports our proposition [26].

Our developed deep-learning models automatically determine the foot posture index for the modified root technique and the necessity of heel lift, entire lift, and lateral wedge, medial wedge, and calcaneocuboid arch supports. The modified root technique considers forefoot-to-rearfoot structural problems and attempts to hold the rearfoot in its neutral position while maintaining the appropriate forefoot-to-rearfoot relation [27–29]. This technique modifies the ground reaction force around the subtalar joint axis [27–29]. The foot posture index is the amount of twisting of the insole to place the rear foot in a neutral position. Heel lift and entire lift are used when the right and left pelvic heights are different [30,31]. In addition, when the side of the pelvic elevation is tilted anteriorly, a heel lift is applied to the other side. When the side of pelvic elevation is not tilted anteriorly, entire lift is applied. Lateral and medial wedge supports are applied to reduce varus and valgus torques, respectively, during walking [14,15]. A calcaneocuboid arch support is used when either side of the pelvis moves backward. A calcaneocuboid arch support is applied

to the side on which the pelvis moves more backward than forward. These prescriptions can be helpful for correcting the malalignment of the lower extremities, as they would effectively reduce pain due to malalignment that occurs in any part of the leg, not only limited to the foot.

When prescribing orthotic insoles, clinicians should consider all the data of the RCSP and the static and dynamic states of the pelvis. Without a deep-learning model, clinicians should prescribe orthotic insoles by considering all these results. Therefore, for the appropriate prescription for patients with foot pain, a lot of experience in the field of foot pain and orthotic insoles is necessary. Incorrect prescription leads to the application of inappropriate insoles, which can aggravate patients' foot pain. We used data on insole prescriptions written by podiatrists with abundant experience in prescribing insoles. We believe that the automatic prescription deep-learning model that we developed can relieve the burden on clinicians of appropriately prescribing orthotic insoles.

The DNN model was trained using an artificial neural network structure based on the neural network structure of the human brain [32]. A DNN is a powerful machine learning algorithm that is implemented by stacking hidden layers of neural networks between the input and output layers [20,21]. It attempts high-level abstraction by combining several non-linear transformations [33]. Deep learning uses a large amount of data for training and creating a model capable of processing new data [34]. It has been used to produce advanced results in various fields, including computer vision, natural language processing, voice recognition, and signal/voice processing [33]. The widely recognized benefits of deep learning include its ability to identify interactions between multiple variables and detect useful information in time series, clinical, and imaging data [35]. In particular, deep learning is more useful for analyzing big data and detecting useful information from images [35]. Deep learning can detect rules or relationships among large amounts of data that cannot be found using traditional statistical analysis methods. The DNN detects the correct mathematical manipulation to convert the input into output through a series of hidden layers [20,21]. When input data are fed into a DNN, the input value is multiplied by the weights at the nodes that comprise each layer, and the output data are generated using an activation function [33].

Parameters such as learning rate, loss function, optimizer, number of epochs and iterations, and batch size are varied by researchers and developers to generate a DNN. An optimal model is determined by evaluating and comparing the accuracy and capacity of each developed model [36,37]. Complex networks with multiple layers effectively represent the complex nature of input and output variables [33]. This feature of DNNs enables the analysis of large amounts of clinical data [36,37]. Multiple layers of a DNN appear to be effective in determining the complex nature of orthotic insole prescription in patients with foot pain.

The procedure for developing a deep-learning algorithm with a large amount of clinical data as the input is as follows: First, the clinical data for deep learning are collected. The clinical data are divided into input and target data and then arranged and saved as comma-separated value files [38]. Programming languages such as Python and R and Python-based deep-learning frameworks such as TensorFlow, PyTorch, and Keras are commonly used to develop deep-learning algorithms [39]. The data, divided into input and target data, are loaded onto the platform and converted into the NumPy array format for deep-learning analysis [39]. Subsequently, the data are stacked in a column and standardized. The data are then divided into training and test datasets, and a deep-learning model is trained [39]. The accuracy of the developed deep-learning model is assessed, and the results are usually depicted by the ROC and AUC [39].

In conclusion, we developed DNN models that automatically prescribe orthotic insoles in patients with foot pain. We demonstrated that their accuracies ranged from outstanding to acceptable. However, for the application of our models in real clinical practice, the accuracy of the prescription of orthotic insoles should be further increased. To increase accuracy, more appropriate input and output data are required. In addition, to increase

the generosity of the models, data or information on the prescription of insoles from more clinicians or podiatrists should be used for the development of models. Finally, the clinical data used to develop the deep-learning models, including RCSP, pelvic elevation, pelvic tilt, and pelvic rotation, were measured manually and visually. However, their reliability and validity have yet to be well-demonstrated. Therefore, a method or tool that can objectively and accurately measure such data must be developed. Further studies are warranted to address these limitations.

Supplementary Materials: The following supporting information can be downloaded at: <https://www.mdpi.com/article/10.3390/app13042208/s1>. Source codes of DNN models.

Author Contributions: J.K.K.: data analysis, data curation, and writing the manuscript; Y.J.C.: data curation; I.S.P.: data curation and preparing figures; J.-W.C.: data curation; D.P.: writing and reviewing the manuscript and preparing figures; M.C.C.: writing and reviewing the manuscript, data analysis, and data curation. All authors have read and agreed to the published version of the manuscript.

Funding: This work was supported by the 2022 Yeungnam University Research Grant.

Institutional Review Board Statement: The study was conducted in accordance with the Declaration of Helsinki, and approved by the Institutional Review Board of Yeungnam University Hospital (2022-06-046).

Informed Consent Statement: Patient consent was waived due to the retrospective nature of our study.

Data Availability Statement: The datasets used and/or analyzed during the current study are available from the corresponding author upon reasonable request.

Conflicts of Interest: The authors declare no conflict of interest.

References

1. Choo, Y.J.; Park, C.H.; Chang, M.C. Rearfoot disorders and conservative treatment: A narrative review. *Ann. Palliat. Med.* **2020**, *9*, 3546–3552.
2. Park, C.H.; Chang, M.C. Forefoot disorders and conservative treatment. *Yeungnam Univ. J. Med.* **2019**, *36*, 92–98. [[CrossRef](#)]
3. Alqahtani, T.A. The prevalence of foot pain and its associated factors among Saudi school teachers in Abha sector, Saudi Arabia. *Family Med Prim Care.* **2020**, *9*, 4641–4647.
4. Chang, M.C. The blind spot and challenges in pain management. *J. Yeungnam Med. Sci.* **2022**, *39*, 179–180.
5. Park, C.H.; Boudier-Revéret, M.; Chang, M.C. Tarsal tunnel syndrome due to talocalcaneal coalition. *Yeungnam Univ. J. Med.* **2023**, *40*, 106–108. [[CrossRef](#)]
6. Chow, T.H.; Chen, Y.S.; Hsu, C.C. Relationships between Plantar Pressure Distribution and Rearfoot Alignment in the Taiwanese College Athletes with Plantar Fasciopathy during Static Standing and Walking. *Int. J. Environ. Res. Public Health* **2021**, *18*, 12942.
7. Menz, H.B.; Dufour, A.B.; Riskowski, J.L.; Hillstrom, H.J.; Hannan, M.T. Association of planus foot posture and pronated foot function are associated with foot pain: The Framingham foot study. *Arthritis Care Res.* **2013**, *65*, 1991–1999.
8. Elattar, O.; Smith, T.; Ferguson, A.; Farber, D.; Wapner, K. Uses of Braces and Orthotics for Conservative Management of Foot and Ankle Disorders. *Foot Ankle Orthop.* **2018**, *3*, 2473011418780700. [[CrossRef](#)]
9. Razeghi, M.; Batt, M.E. Biomechanical analysis of the effect of orthotic shoe inserts: A review of the literature. *Sports Med.* **2000**, *29*, 425–438. [[CrossRef](#)]
10. Amer, A.O.; Jarl, G.M.; Hermansson, L.N. The effect of insoles on foot pain and daily activities. *Prosthet. Orthot. Int.* **2014**, *38*, 474–480.
11. Gómez Carrión, Á.; Atín Arratibe, M.L.Á.; Morales Lozano, M.R.; Martínez Rincón, C.; Martínez Sebastián, C.; Saura Sempere, Á.; Nuñez-Fernandez, A.; Sánchez-Gómez, R. Changes in the Kinematics of Midfoot and Rearfoot Joints with the Use of Lateral Wedge Insoles. *J. Clin. Med.* **2022**, *11*, 4536.
12. Paterson, K.L.; Hinman, R.S.; Metcalf, B.R.; McManus, F.; Jones, S.E.; Menz, H.B.; Munteanu, S.E.; Bennell, K.L. Effect of foot orthoses vs sham insoles on first metatarsophalangeal joint osteoarthritis symptoms: A randomized controlled trial. *Osteoarthritis Cartil.* **2022**, *30*, 956–964.
13. Khamis, S.; Dar, G.; Peretz, C.; Yizhar, Z. The Relationship Between Foot and Pelvic Alignment While Standing. *J. Hum. Kinet.* **2015**, *46*, 85–97. [[CrossRef](#)]
14. Fukuchi, C.A.; Lewinson, R.T.; Worobets, J.T.; Stefanyshyn, D.J. Effects of Lateral and Medial Wedged Insoles on Knee and Ankle Internal Joint Moments During Walking in Healthy Men. *J. Am. Podiatr. Med. Assoc.* **2016**, *106*, 411–418. [[CrossRef](#)]

15. Kerrigan, D.C.; Lelas, J.L.; Goggins, J.; Merriman, G.J.; Kaplan, R.J.; Felson, D.T. Effectiveness of a lateral-wedge insole on knee varus torque in patients with knee osteoarthritis. *Arch. Phys. Med. Rehabil.* **2002**, *83*, 889–893.
16. Mahmoud, A.; Abundo, P.; Basile, L.; Albensi, C.; Marasco, M.; Bellizzi, L.; Galasso, F.; Foti, C. Functional leg length discrepancy between theories and reliable instrumental assessment: A study about newly invented NPoS system. *Muscles Ligaments Tendons J.* **2017**, *7*, 293–305.
17. Choo, Y.J.; Kim, J.K.; Kim, J.H.; Chang, M.C.; Park, D. Machine learning analysis to predict the need for ankle foot orthosis in patients with stroke. *Sci. Rep.* **2021**, *11*, 8499. [[CrossRef](#)]
18. Kim, J.K.; Choo, Y.J.; Chang, M.C. Prediction of Motor Function in Stroke Patients Using Machine Learning Algorithm: Development of Practical Models. *J. Stroke Cerebrovasc. Dis.* **2021**, *30*, 105856.
19. Kim, J.K.; Lv, Z.; Park, D.; Chang, M.C. Practical Machine Learning Model to Predict the Recovery of Motor Function in Patients with Stroke. *Eur. Neurol.* **2022**, *85*, 273–279.
20. Kim, J.K.; Chang, M.C.; Park, D. Deep Learning Algorithm Trained on Brain Magnetic Resonance Images and Clinical Data to Predict Motor Outcomes of Patients With Corona Radiata Infarct. *Front. Neurosci.* **2022**, *15*, 795553.
21. Shin, H.; Choi, G.S.; Shon, O.J.; Kim, G.B.; Chang, M.C. Development of convolutional neural network model for diagnosing meniscus tear using magnetic resonance image. *BMC Musculoskelet. Disord.* **2022**, *23*, 510. [[CrossRef](#)]
22. Cho, Y.; Park, J.W.; Nam, K. The relationship between foot posture index and resting calcaneal stance position in elementary school students. *Gait Posture* **2019**, *74*, 142–147. [[CrossRef](#)]
23. Keenan, A.M.; Bach, T.M. Clinicians' assessment of the hindfoot: A study of reliability. *Foot Ankle Int.* **2006**, *27*, 451–460. [[CrossRef](#)]
24. Kouhkan, S.; Rahimi, A.; Ghasemi, M.; Naimi, S.S.; Baghban, A.A. Postural Changes during First Pregnancy. *Br. J. Med. Med. Res.* **2015**, *7*, 744–753. [[CrossRef](#)]
25. Wang, S.; Minku, L.L. AUC estimation and concept drift detection for imbalanced data streams with multiple classes. In Proceedings of the 2020 International Joint Conference on Neural Networks (IJCNN), Glasgow, UK, 19–24 July 2020; pp. 1–8.
26. Mandrekar, J.N. Receiver operating characteristic curve in diagnostic test assessment. *J. Thorac. Oncol.* **2010**, *5*, 1315–1316. [[CrossRef](#)]
27. Buchanan, K.R.; Davis, I. The relationship between forefoot, midfoot, and rearfoot static alignment in pain-free individuals. *J. Orthop. Sports Phys. Ther.* **2005**, *35*, 559–566.
28. Kim, P.J.; Peace, R.; Mieras, J.; Thoms, T.; Freeman, D.; Page, J. Interrater and intrarater reliability in the measurement of ankle joint dorsiflexion is independent of examiner experience and technique used. *J. Am. Podiatr. Med. Assoc.* **2011**, *101*, 407–414.
29. Menz, H.B. Foot orthoses: How much customisation is necessary? *J Foot Ankle Res.* **2009**, *2*, 23. [[CrossRef](#)]
30. Severin, A.C.; Gean, R.P.; Barnes, S.G.; Queen, R.; Butler, R.J.; Martin, R.; Barnes, C.L.; Mannen, E.M. Effects of a corrective heel lift with an orthopaedic walking boot on joint mechanics and symmetry during gait. *Gait Posture* **2019**, *73*, 233–238.
31. Yen, S.T.; Andrew, P.D.; Cummings, G.S. Short-term effect of correcting leg length discrepancy on performance of a forceful body extension task in young adults. *Hiroshima J. Med. Sci.* **1998**, *47*, 139–143.
32. Kriegeskorte, N.; Golan, T. Neural network models and deep learning. *Curr. Biol.* **2019**, *29*, R231–R236.
33. Sarker, I.H. Deep learning: A comprehensive overview on techniques, taxonomy, applications and research directions. *SN Comput. Sci.* **2021**, *2*, 420. [[CrossRef](#)]
34. LeCun, Y.; Bengio, Y.; Hinton, G. Deep learning. *Nature* **2015**, *521*, 436–444.
35. Rajula, H.S.; Verlato, G.; Manchia, M.; Antonucci, N.; Fanos, V. Comparison of conventional statistical methods with machine learning in medicine: Diagnosis, drug development, and treatment. *Medicina* **2020**, *56*, 455. [[CrossRef](#)]
36. Choo, Y.J.; Chang, M.C. Use of Machine Learning in Stroke Rehabilitation: A Narrative Review. *Brain Neurorehabil.* **2022**, *15*, e26.
37. Lee, H.; Song, J. Introduction to convolutional neural network using Keras; an understanding from a statistician. *Commun. Stat. Appl. Methods* **2019**, *26*, 591–610. [[CrossRef](#)]
38. Giulia, A.; Anna, S.; Antonia, B.; Dario, P.; Maurizio, C. Extending association rule mining to microbiome pattern analysis: Tools and guidelines to support real applications. *Front. Bioinform.* **2022**, *1*, 794547. [[CrossRef](#)]
39. Mendez, K.M.; Pritchard, L.; Reinke, S.N.; Broadhurst, D.I. Toward collaborative open data science in metabolomics using Jupyter Notebooks and cloud computing. *Metabolomics* **2019**, *15*, 125. [[CrossRef](#)]

Disclaimer/Publisher's Note: The statements, opinions and data contained in all publications are solely those of the individual author(s) and contributor(s) and not of MDPI and/or the editor(s). MDPI and/or the editor(s) disclaim responsibility for any injury to people or property resulting from any ideas, methods, instructions or products referred to in the content.